Smoothed density of states of electrons and smoothed frequency spectrum of phonons for a mesoscopic system

Akira Tamura
Department of Electronic Engineering, Saitama Institute of Technology, 1690 Fusaiji, Okabe-machi, Ohsato-gun, 369-02 Saitama, Japan
(Received 2 February 1995)

For the finite systems of a sphere, a disk, a linear line, and a tube, the smoothed electron density of states (DOS) is derived directly from the distribution of eigenvalues of a one-particle model. The smoothed DOS is defined by setting one of the quantum numbers to a continuous variable. For a spherical particle, the DOS is expressed as the sum of three terms; a volume term, a surface term, and a circumference term. We clarify the changes in the DOS between a mesoscopic system and a macroscopic system. We apply the same method to phonons of a mesoscopic system and derive the smoothed frequency spectrum.

I. INTRODUCTION

In recent years mesoscopic systems have been the focus of attention in many fields, not only in physical science but also in electronics. It has been shown that the finite size affects many kinds of physical and chemical properties.[1–3] Electrons have discrete energy levels and the discreteness is decisive for the stable structure of microclusters. Degeneracy of energy levels plays an important role in accommodating electrons from the lowest level to the Fermi energy. As a typical example it has been observed that the ionization potential of microclusters is oscillatory as a function of the number of atoms.[2,3] The numbers of atoms that close discrete energy shells are called magic numbers in a similar manner to the stable nuclei.

The electron density of states (DOS) reflects the structure of electron energy levels and the degeneracy. In this paper we derive the smoothed DOS directly from the distribution of eigenenergies and compare our DOS with that obtained by Balian and Bloch.[4–7] We elucidate the trend that the DOS of a three-dimensional (3D) system becomes proportional to $\sqrt{E}$ with the increase in cluster size.

The phonons of a mesoscopic system are characterized by discrete vibrational frequencies, which are responsible for the thermodynamic properties; the specific heat[8–10] and the mean square displacements of vibrating atoms.[11–13] These quantities are larger than those of the bulk system because of the surface mode contribution. A fundamental quantity that specifies the thermodynamic properties of materials is the phonon frequency spectrum (FS).[14,15] We derive the smoothed FS directly from the distribution of eigenfrequencies and clarify the trend that the FS in the low-frequency range becomes proportional to ω^2 with increase in system size.

II. SMOOTHED DOS FOR ELECTRONS

Since Weyl's work,[16] the effect of boundary conditions on eigenvalues and on the DOS has been investigated. For a spherical particle, Balian and Bloch[4] derived the smoothed DOS. They treated the boundary-value problem for the following partial differential equation:

$$\Delta\phi + k^2\phi = 0 , \tag{1}$$

with the surface boundary condition that

$$\nabla_n \phi = \kappa\phi , \tag{2}$$

where κ is a constant and the subscript n represents the derivative in the direction normal to the surface. They obtained the smoothed DOS in the limit of large wave number by using the Green's function and Lorentzian smooth method:

$$D_\gamma(E) = \frac{m}{\pi^2\hbar^2}\left[Vk + S\left(\frac{\pi}{4} - \delta\right) + \frac{2L}{k}\left(\tfrac{1}{3} + \cos^2\delta - \delta\cot\delta\right) + \cdots \right] , \tag{3}$$

where E is the energy, V is the volume, S is the area, and L is the circumference. The parameter δ is defined by

$$\delta = \arctan\left(\frac{\kappa}{k}\right) , \tag{4}$$

with

$$k = \left(\frac{2mE}{\hbar^2}\right)^{1/2} . \tag{5}$$

In the limit $\kappa = \infty$ the boundary condition corresponds to a fixed boundary condition and $\kappa = 0$ to a free boundary condition. $D_\gamma(E)$ has the volume term $\sqrt{E}$, the surface term a constant, and the circumference term $1/\sqrt{E}$. Moreover, Balian and Bloch[7] revealed an oscillatory feature of the DOS that is called a supershell.[17,18] The smoothed DOS becomes the basis when we consider shell effects on the fragmentation process of a charged alkali-metal cluster.[19]

In many cases we calculate eigenvalues with various

boundary conditions which are more complex than that of Eq. (2). It is necessary, therefore, to obtain the DOS directly from the distribution of eigenvalues. On this point the present theory is different from that by Balian and Bloch.[4-7]

We describe the eigenstates of the system by good quantum numbers that characterize the symmetry property of the system. For a spherical system, a good quantum number is the angular momentum, while the wave vector is a good quantum number for a system that has translational symmetry. Here we focus on the sphere and derive the energy levels for a one-particle model. Assuming that the potential is a square-well type with an infinite wall, we obtain the energy levels from the zeros of the spherical Bessel functions,

$$j_l(\eta)=0 , \tag{6}$$

$$E_{nl}=\frac{\hbar^2}{2mR^2}\eta_{nl}^2 , \tag{7}$$

where n represents the branch number, l represents the angular momentum, η_{nl} is the reduced eigenvalue, and R is the radius. Figure 1 shows a diagram for η_{nl}. Since the degeneracy of the lth state is $(2l+1)$, the number of states included in the range between E and $E+\delta E$ is proportional to $(2l+1)\delta l$ for a certain branch n. Thus we define the smoothed DOS by

$$\bar{D}^{(3)}_{\rm fix}(E)\delta E=2\sum_n (2l+1)\delta l , \tag{8}$$

where the factor 2 is the spin degree of freedom. By writing approximately the series of reduced eigenvalues as

$$\eta_{nl}=\alpha l+\beta n , \tag{9}$$

in the low-energy range and noting that

$$\delta E=\frac{\hbar^2}{mR^2}\eta\delta\eta , \tag{10}$$

we find

$$(2l+1)\delta l=\frac{2mR^2}{\hbar^2\alpha^2}\frac{(\eta+\alpha/2-\beta n)}{\eta}\delta E \tag{11}$$

for a fixed n. We take the sum over n in Eq. (8) to the maximum N that satisfies

$$\eta+\frac{\alpha}{2}-\beta N=0 . \tag{12}$$

The integer N means the number of segments of the reduced eigenvalue. Thus we obtain the smoothed DOS as

$$\bar{D}^{(3)}_{\rm fix}(E)=\frac{3}{4\pi\alpha^2\beta}\left[\frac{2m}{\hbar^2}\right]^{3/2} \times\left\{V\sqrt{E}+\frac{S}{3}\left[\frac{\hbar}{2m}\right]^{1/2}(\alpha-\beta) +\frac{L}{6}\left[\frac{\hbar^2}{2m}\right]\alpha(\alpha-2\beta)\frac{1}{\sqrt{E}}\right\} . \tag{13}$$

The value β corresponds to the area of a parallelogram surrounded by neighboring segments of angular momenta and neighboring segments of branch numbers. The second term shows the surface contribution and the third term shows the circumference contribution. If the dimensionless parameter $2mR^2E/\hbar^2\gg 1$ (large size and/or high energy) $\bar{D}^{(3)}_{\rm fix}(E)$ leads to the DOS of the bulk system. We should note that the three terms have different energy dependence. This comes from the dimensionality of the system; $\sqrt{E}$ of the 3D bulk system, a constant of the 2D bulk system, and $1/\sqrt{E}$ of the 1D bulk system. We discuss the DOS of low-dimensional systems in Sec. III.

Figure 2 shows schematically the contribution from each branch to $\bar{D}^{(3)}_{\rm fix}(E)$. The thick curve shows the superposed DOS and the thin curves show the contributions from each branch. Evidently the superposition is responsible for the trend of the change of the DOS from a microsystem to a macrosystem. If the system size decreases, the segment of energy becomes large, and

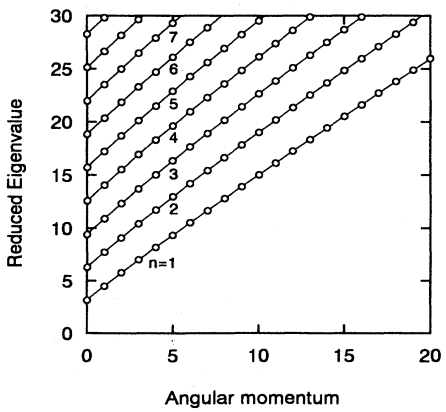

FIG. 1. Distribution of eigenvalues derived with a fixed boundary condition at a spherical surface. Open circles show eigenvalues.

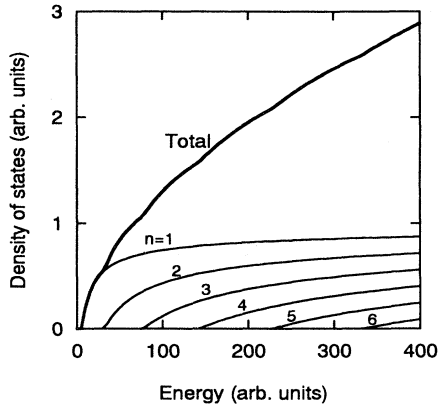

FIG. 2. Schematic diagram for the smoothed DOS. The thick curve shows the superposed DOS and the thin curves show the contributions from each branch. Inserted figures represent branch numbers.

$\bar{D}^{(3)}_{\rm fix}(E)$ becomes rough because of the finiteness of the system. With an increase in the system size, the segment becomes small, and $\bar{D}^{(3)}_{\rm fix}(E)$ becomes smooth and closer to the DOS of the bulk system,

$$D^{(3)}_{\rm bulk}(E)=\frac{V}{2\pi^2}\left[\frac{2m}{\hbar^2}\right]^{3/2}\sqrt{E}\ . \tag{14}$$

Two parameters α and β must, therefore, satisfy the following equation:

$$\alpha^2\beta=\frac{3\pi}{2}\ . \tag{15}$$

In the present case $\alpha=1.22$, $\beta=3.14$, and $\gamma=0$. The coefficient of the second term of Eq. (13) is calculated as $(\alpha-\beta)/3=-0.64$ and the coefficient of the third term is calculated as $\alpha(\alpha-2\beta)/6=-1.03$. Those by Balian and Bloch[4] are -0.79 and 0.67, respectively. Figure 3 shows the DOS and Fig. 4 shows the DOS in the low-energy range. Though the coefficient of the second term calculated by Balian and Bloch[4] is less than ours, their DOS is higher than ours. This indicates that the third term in Eq. (13) is not negligible in the low-energy range. Thus our DOS is better than that by Balian and Bloch[4] since their DOS is slightly higher than the middle points of the indented histogram (Fig. 4) because of the positive coefficient of the third term.

For a free-boundary condition at the surface that

$$\nabla_n\phi=0\ , \tag{16}$$

the distribution of eigenvalues differs from that for a square well with an infinite wall. Figure 5 shows the distribution of eigenvalues as a function of angular momentum. By writing the eigenvalues approximately as

$$\eta_{nl}=\alpha l+\beta n+\gamma\ , \tag{17}$$

we have the following smoothed DOS in the same way as above:

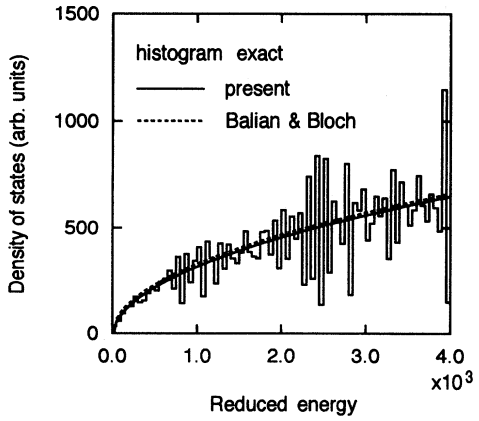

FIG. 3. Electron DOS for eigenvalues of a sphere calculated with a fixed boundary condition. The segment of reduced energy is set to be 50. The dashed curve shows the smoothed DOS calculated by Eq. (3) (Ref. 4).

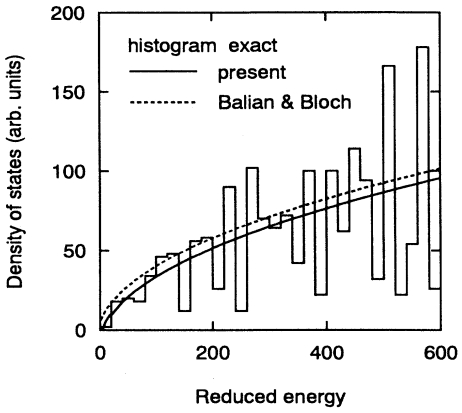

FIG. 4. Electron DOS for low eigenvalues of a sphere calculated with a fixed boundary condition. The segment of reduced energy is set to be 20. The dashed curve shows the smoothed DOS calculated by Eq. (3) (Ref. 4).

$$\bar{D}^{(3)}_{\rm free}(E)=\frac{3}{4\pi\alpha^2\beta}\left[\frac{2m}{\hbar^2}\right]^{3/2}\times\left\{V\sqrt{E}+\frac{S}{3}\left[\frac{\hbar^2}{2m}\right]^{1/2}(\alpha-\beta-2\gamma)+\frac{L}{6}\left[\frac{\hbar^2}{2m}\right](\alpha-2\gamma)(\alpha-2\beta-2\gamma)\frac{1}{\sqrt{E}}\right\}. \tag{18}$$

$\bar{D}^{(3)}_{\rm free}(E)$ is expanded in terms of R^{-1} in the same way as $\bar{D}^{(3)}_{\rm fix}(E)$. The factor γ modifies the coefficients of the surface and circumference terms in Eq. (13). The bulk term is the same as that of $\bar{D}^{(3)}_{\rm fix}(E)$ since it must be independent of the boundary conditions, that is, $\bar{D}^{(3)}_{\rm free}(E)$ is proportional to $\sqrt{E}$ for an infinite radius of a sphere.

Figure 6 shows the DOS. The coefficient of the surface term is positive since $\alpha=1.22$, $\beta=3.14$, and $\gamma=-1.79$. The reason is that a free boundary condition results in

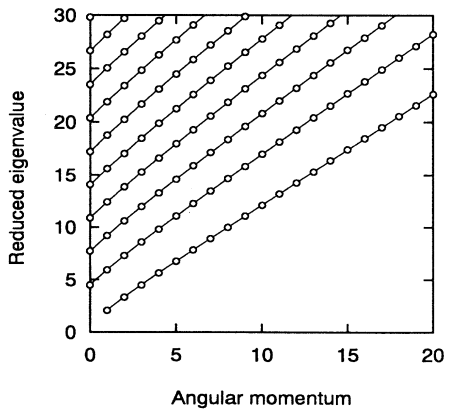

FIG. 5. Distribution of eigenvalues derived with a free boundary condition at a spherical surface.

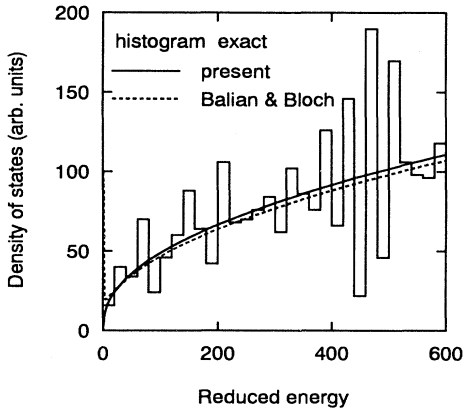

FIG. 6. Electron DOS for low eigenvalues of a sphere calculated with a free boundary condition. The segment of reduced energy is set to be 20. The dashed curve shows the smoothed DOS calculated by Eq. (3) (Ref. 4).

finite wave functions at the surface, while a fixed boundary condition makes the wave functions null at the surface. If electrons are confined in an infinite wall, the wave functions are compressed into the inner region, which reduces the surface states' contribution. Thus a free boundary condition yields surface states which make a positive contribution to $\bar{D}^{(3)}_{\text{free}}(E)$. The coefficients of $\bar{D}^{(3)}_{\text{free}}(E)$ are calculated so that $(\alpha-\beta-2\gamma)/3=0.55$ (the second term) and

$$(\alpha-2\gamma)(\alpha-2\beta-2\gamma)/6=-1.18$$

(the third term), while those by Balian and Bloch[4] are 0.79 and 2.67, respectively. We should note that the $D_\gamma(E)$ obtained by Balian and Bloch[4] is infinite at $E=0$ in contrast to the exact distribution of eigenvalues, which has an energy gap between $E=0$ and the lowest eigenenergy. We should notice that their theory is based on a large-k expansion.

III. 2D AND 1D SYSTEMS

We consider the smoothed DOS of two-dimensional and one-dimensional systems in the same way. As an example of 2D systems, we focus on a spherical disk. With a fixed boundary condition, we derive the eigenvalues from the zeros of the Bessel function of the first kind $J_l(\eta)$. In the same way as in Eq. (7), the eigenvalues are specified by angular momentum l and branch number n. We define the smoothed DOS as the summation of δn over l:

$$\bar{D}^{(2)}(E)\delta E=4\sum_{l=1}\delta n+2\delta n\ , \tag{19}$$

where the factor 4 on the right comes from the contribution from the spin degree of freedom and the degeneracy associated with magnetic quantum numbers $m=\pm l$. We should note that the state with $l=0$ has only a spin degree of freedom. The second term in Eq. (19) represents this correction. With the approximate expression

$$\eta_{nl}=\alpha l+\beta n+\gamma \tag{20}$$

and the relation

$$\delta n=\frac{1}{\beta}\delta\eta\ , \tag{21}$$

we obtain the smoothed DOS

$$\bar{D}^{(2)}(E)=\frac{4m}{\pi\hbar^2\alpha\beta}\left\{S+\frac{L}{4}\left[\frac{\hbar^2}{2m}\right]^{1/2}(\alpha-2\beta-2\gamma)\frac{1}{\sqrt{E}}\right\}\ , \tag{22}$$

where S is the area of the spherical disk and L is the circumference. Discreteness of the eigenvalues is retained in the summation over l, which is different from the 3D case in Sec. II, with summation over n. The DOS of the 2D bulk system is

$$D^{(2)}_{\text{bulk}}(E)=\frac{mS}{\pi\hbar^2}\ , \tag{23}$$

which is independent of E. Since our smoothed DOS must reproduce the DOS of the 2D bulk system in the case of an infinite radius, the parameters α and β introduced in Eq. (20) must satisfy $\alpha\beta=4$. The term proportional to $1/\sqrt{E}$ in Eq. (22) represents the contribution from the circumference.

Figure 7 shows the DOS determined by a fixed boundary condition on electrons. The supershell structure appears around a constant line and the oscillation becomes striking as the energy segment of the histogram decreases. Our DOS is less than the average value ($=50$ in the present case), especially in the low-energy range, which is consistent with the exact DOS. This indicates that the second term of Eq. (22) is not negligible in the low-energy range.

As an example of 1D systems, we consider a finite line of length L. With fixed boundary conditions at the two ends, we obtain the eigenenergies of electrons from the zeros of $\sin\eta$: $\eta_n=n\pi$. Since the system has only one

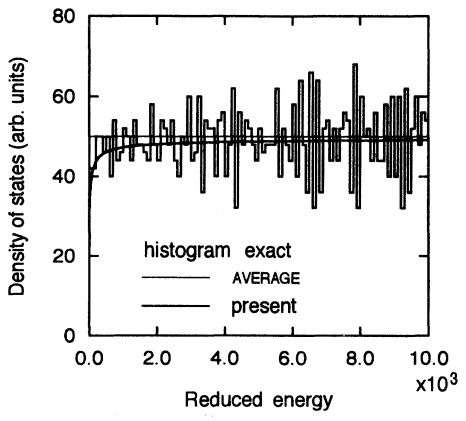

FIG. 7. Electron DOS for eigenvalues of a spherical disk with a fixed boundary condition. The segment of reduced energy is set to be 100.

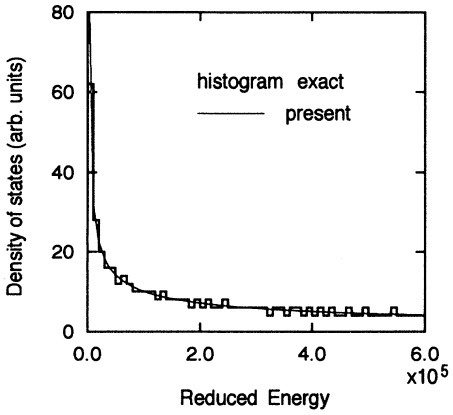

FIG. 8. Electron DOS for eigenvalues of a line with a fixed boundary condition. The segment of reduced energy is set to be 10 000.

quantum number n, we define the smoothed DOS by

$$\bar{D}^{(1)}_{\rm fix}(E)\delta E = 2\delta n \ . \tag{24}$$

In the same way as for the 2D and 3D cases, we find the smoothed DOS:

$$\bar{D}^{(1)}_{\rm fix}(E) = \frac{L}{\pi}\left[\frac{2m}{\hbar^2}\right]^{1/2}\frac{1}{\sqrt{E}} \ . \tag{25}$$

This is exactly the DOS of the 1D bulk system because η_n is specified by only one parameter n. Figure 8 shows the DOS of the 1D bulk system and the smoothed DOS of the finite system. Clearly, our DOS is in the middle of the indented region of the histogram in a wide range.

Next we consider a tube of radius R and length H. We impose a periodic boundary condition on the angular component of the wave function and fixed boundary conditions at the two ends of the axial component. We find the following energy levels:

$$E_{nj} = \frac{\hbar^2}{2mR^2}n^2 + \frac{\pi^2\hbar^2}{2mH^2}j^2 \ , \tag{26}$$

where n is an integer and j is a natural number. The number n corresponds to the angular momentum around the center axis of a tube. We define the smoothed DOS by

$$\begin{aligned}\bar{D}^{\rm tube}(E)\delta E &= 4\sum_{n=1}^{n_{\max}}\delta j \\ &= 2\left[\frac{2mH^2}{\pi^2\hbar^2}\right]^{1/2} \\ &\quad\times\sum_{n=1}^{n_{\max}}\frac{1}{\sqrt{E-(\hbar^2/2mR^2)n^2}}\delta E \ ,\end{aligned} \tag{27}$$

where

$$n_{\max} = \left[\frac{2mR^2}{\hbar^2}E - \left[\frac{\pi R}{H}\right]^2\right]^{1/2} \ . \tag{28}$$

$\bar{D}^{\rm tube}(E)$ is expressed as the summation of $\bar{D}^{(1)}_{\rm fix}(E)$ with energy shifts $\hbar^2n^2/(2mR^2)$. The parameter $n_{\max}$ is introduced to eliminate states with $j=0$. We transform the summation in Eq. (27) into the integral

$$\begin{aligned}\bar{D}^{\rm tube}(E) &= 2\left[\frac{2mH^2}{\pi^2\hbar^2}\right]^{1/2}\int_1^{n_{\max}}\frac{1}{\sqrt{E-(\hbar^2/2mR^2)n^2}}dn \\ &= \frac{2mS}{\pi^2\hbar^2}\arcsin\left[\left[1-\frac{\hbar^2}{2mR^2E}\right]^{1/2}\left[1-\frac{\pi^2\hbar^2}{2mH^2E}\right]^{1/2} - \frac{\pi\hbar^2}{2mRHE}\right] \ .\end{aligned} \tag{29}$$

This equation is symmetric with respect to interchange of R and H/π. By expanding $\bar{D}^{\rm tube}(E)$ at large E we have the asymptotic expression

$$\bar{D}^{\rm tube}(E) = \frac{mS}{\pi\hbar^2}\left[1-2\left[\frac{\hbar^2}{2m}\right]^{1/2}\left[1+\frac{\pi R}{H}\right]\frac{1}{L}\frac{1}{\sqrt{E}}\right] \ , \tag{30}$$

where $L=2\pi R$. To make clear the feature of this system, we expand Eq. (30) to

$$\begin{aligned}\bar{D}^{\rm tube}(E) &= \frac{mS}{\pi\hbar^2} - 2\frac{H}{\pi}\left[\frac{2m}{\hbar^2}\right]^{1/2}\frac{1}{\sqrt{E}} \\ &\quad - \frac{L}{\pi}\left[\frac{2m}{\hbar^2}\right]^{1/2}\frac{1}{\sqrt{E}} \ .\end{aligned} \tag{31}$$

The first term shows the DOS of the 2D bulk system. The second term shows the DOS of a 1D system of length H and the third term shows the DOS of a 1D system of length L. The coefficient 2 of the second term comes from the contributions from two ends of a tube and the negative sign represents elimination of states with $n=0$. On the other hand, the negative sign of the third term represents elimination of states with $j=0$. This situation is ascribable to the effect of the boundary conditions; the quantum number j for fixed boundary conditions at the two ends and the quantum number n from the periodic boundary condition around a tube. Even if we consider the variation δn instead of δj, we arrive at the same result from the following definition:

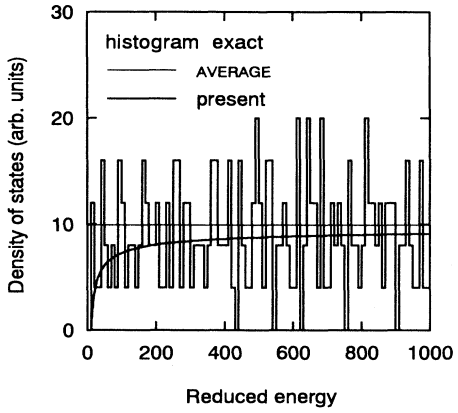

FIG. 9. Electron DOS for eigenvalues of a tube. The parameter $(\pi R/H)^2=10$. The segment of reduced energy is set to be 10.

$$\overline{D}^{\,\mathrm{tube}}(E)\delta E=2\sum_{j=1}^{j_{\max}}\delta n$$
$$=2\left[\frac{2mR^2}{\hbar^2}\right]^{1/2}\times\sum_{j=1}^{j_{\max}}\frac{1}{\sqrt{E-(\pi^2\hbar^2/2mH^2)j^2}}\delta E\ , \quad (32)$$

where

$$j_{\max}=\left[\frac{2mH^2}{\pi^2\hbar^2}E-\left[\frac{H}{\pi R}\right]^2\right]^{1/2}\ . \quad (33)$$

It is, therefore, essential to make one of the quantum numbers a continuous variable in order to derive the smoothed DOS. Figure 9 shows the DOS for the case $(\pi R/H)^2=10$. If the ratio R/H is extremely small, that is, an extremely long tube, the DOS approaches the superposed $\overline{D}^{(1)}_{\mathrm{fix}}(E)$ with the energy shifts shown in the denominator of Eq. (27). Figure 10 shows the DOS for the case $(\pi R/H)^2=0.1$. The peaks are located at the squares of the natural numbers 1,4,9,16,25,. . . .

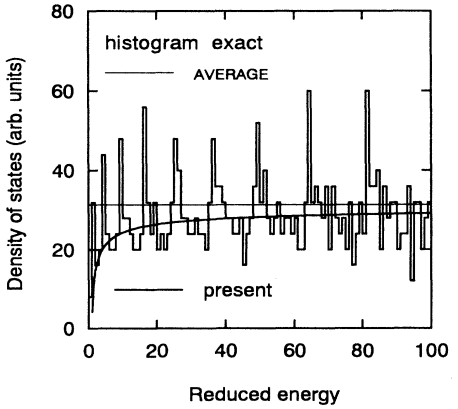

FIG. 10. Electron DOS for eigenvalues of a tube. The parameter $(\pi R/H)^2=0.01$. The segment of reduced energy is set to be 1.

IV. SMOOTHED FS FOR PHONONS

On the basis of an elastic vibration model, we derive the vibrational modes of a finite sphere. The elastic displacement vector $\mathbf{D}$ satisfies the equation

$$\rho\frac{\partial^2}{\partial t^2}\mathbf{D}=(\lambda+\mu)\nabla(\nabla\cdot\mathbf{D})+\mu\nabla^2\mathbf{D}\ , \quad (34)$$

where ρ is the mass density and λ and μ are Lamé's elastic constants. We solve this equation by introducing a scalar potential and a vector potential that satisfy Helmholz's equations.[10] We consider a stress-free boundary condition at the surface and finiteness conditions on both elastic displacements and stresses at the center. These boundary conditions yield two kinds of eigenmodes: the spheroidal mode and the torsional mode. The spheroidal mode is a coupled one composed of longitudinal and transverse displacements. The torsional mode is expressed by one kind of transverse displacement. For the spheroidal mode, we obtain reduced eigenfrequencies from the following eigenvalue equation:

$$2\left\{\eta^2+(l-1)(l+2)\left[\eta\frac{j_{l+1}(\eta)}{j_l(\eta)}-(l+1)\right]\right\}\xi\times\frac{j_{l+1}(\xi)}{j_l(\xi)}-\tfrac{1}{2}\eta^4+[\eta^2-2l(l-1)(l+2)]\eta\frac{j_{l+1}(\eta)}{j_l(\eta)}$$
$$+(l-1)(2l+1)\eta^2=0\ , \quad (35)$$

where $\xi=\omega R/c_l$ and $\eta=\omega R/c_t$. The parameters c_l and c_t are the sound velocities of the longitudinal and transverse modes, respectively. For the torsional mode, we find reduced eigenfrequencies from

$$\frac{d}{d\eta}\left[\frac{j_l(\eta)}{\eta}\right]=0\ . \quad (36)$$

Though the eigenvalues η of the spheroidal mode depend on one material parameter c_l/c_t, those of the torsional

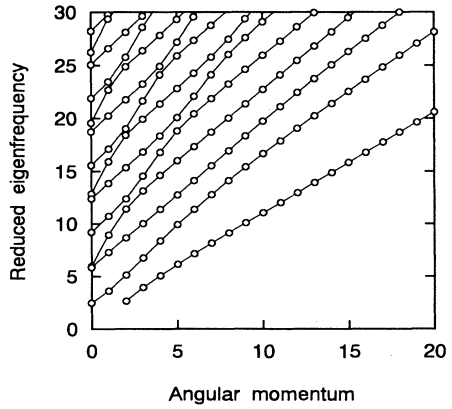

FIG. 11. Distribution of eigenvalues for spheroidal modes. The parameter $c_l/c_t=2.10$.

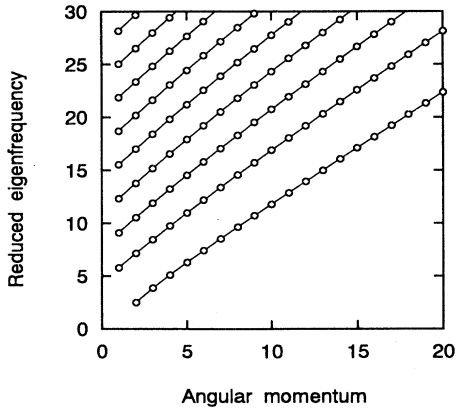

FIG. 12. Distribution of eigenvalues for torsional modes.

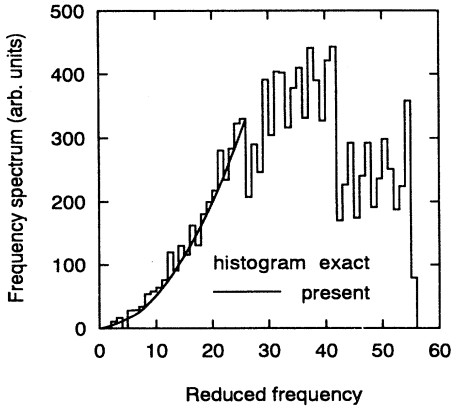

FIG. 13. Phonon FS for a spherical cluster of aluminum. The segment of reduced frequency is set to be 1.

mode have no material dependence. Figures 11 and 12 show the distribution of eigenvalues for the case of aluminum. In Fig. 11 we see two kinds of bunches of lines that come from longitudinal and transverse modes, respectively. Moreover, we see energy repulsion between adjacent points of the longitudinal branches and transverse branches. This is the interaction between longitudinal and transverse modes because of the stress-free boundary condition at the surface. For the details we refer to Tamura, Higeta, and Ichinokawa.[10]

In the same way as in the case of electrons, we define the smoothed FS by

$$\bar{F}(\omega)\delta\omega=\sum_{\sigma}\sum_{n}(2l+1)\delta l\ , \tag{37}$$

and we consider the approximate expression for the reduced eigenfrequency η_{nl}^{σ}

$$\eta_{nl}^{\sigma}=\alpha_{\sigma}l+\beta_{\sigma}n+\gamma_{\sigma}\ , \tag{38}$$

where σ represents the polarization. The phonon frequency is written as

$$\omega_{nl}^{\sigma}=\frac{c_{\sigma}}{R}\eta_{nl}^{\sigma}\ , \tag{39}$$

where c_{σ} is the sound velocity and R is the radius. For simplicity, we split the spheroidal modes into two groups: longitudinal modes with a large inclination and transverse modes with a small inclination. The longitudinal branches have $\alpha=2.56$, $\beta=6.59$, and $\gamma=0$ and the transverse branches have $\alpha=1.22$, $\beta=3.14$, and $\gamma=-3.14$. The difference between these values comes from the ratio c_l/c_t: 2.10 for aluminum. The lowest branch of torsional modes has $\alpha=1.3$ and $\beta=\gamma=0$ and the upper branches have $\alpha=1.22$, $\beta=3.14$, and $\gamma=-3.14$. Spheroidal modes with $l=0$ and $l=1$ of the lowest branch should be eliminated. Moreover, torsional modes with $l=0$ and $l=1$ of the lowest branch should be eliminated. Figure 13 shows the calculated FS for an aluminum cluster. The smoothed FS is in the middle of the indented edges of the exact histogram in the low-frequency range.

Next we discuss how the frequency spectrum of a microsystem changes into that of a macrosystem. If the radius of a mesoscopic system tends to infinity, $F(\omega)$ has to be the bulk one:[20]

$$F_{\sigma}^{\text{bulk}}(\omega)=\frac{V}{2\pi^2c_{\sigma}^3}\omega^2\ . \tag{40}$$

By writing the reduced frequency of a spherical system as

$$\eta_{nl}=\alpha l+\beta n+\gamma\ , \tag{41}$$

we obtain the smoothed FS of the finite system as follows:

$$\begin{aligned}\sum_{n}(2l+1)\delta l&=\frac{2}{\alpha^2}\sum_{n}\left[\eta+\frac{\alpha}{2}-\gamma-\beta n\right]\delta\eta\\&=\frac{1}{\alpha^2\beta}\left[\left[\eta+\frac{\alpha}{2}-\gamma\right]^2-\beta\left[\eta+\frac{\alpha}{2}-\gamma\right]\right]\delta\eta\ .\end{aligned} \tag{42}$$

We should note that the leading term has a quadratic dependence on η and the term to be summed in Eq. (42) is a linear function of η. This is the reason for the ω^2 dependence of the bulk FS in contrast to the case of the electron DOS. Figure 14 shows a schematic diagram of the FS which represents the change from a microsystem to a macrosystem. Further discussion will be reported elsewhere.

V. SMOOTHED FS FOR PHONONS OF A LIQUID DROP

We consider the oscillation modes of a droplet of an irrotational liquid. If the droplet is large, it has two kinds of oscillation modes: shape oscillations induced by the surface tension and compressional oscillations induced by the compressibility. The eigenfrequency of shape oscillations is[21,22]

$${}_s\omega_l=\left[\frac{\gamma_s}{\rho R^3}l(l-1)(l+2)\right]^{1/2}\ , \tag{43}$$

where l is the angular momentum, γ_s is the surface tension, ρ is the mass density, and R is the radius. The dependence on l is different from that of the phonons of a

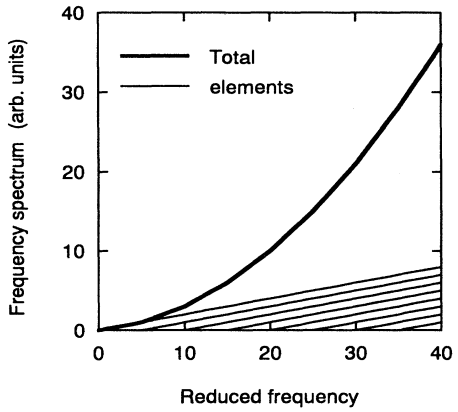

FIG. 14. Schematic diagram for the smoothed FS. The thin curves show the contribution from each branch and the thick curve shows the superposed DOS. As the system size increases, the thick curve becomes smoother.

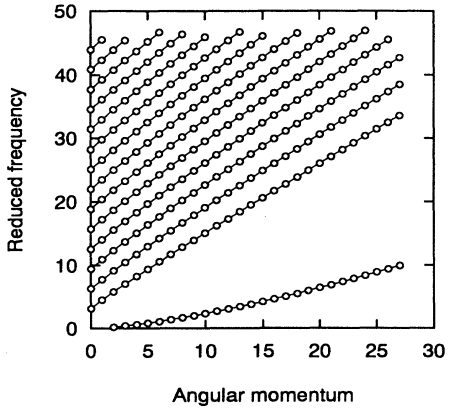

FIG. 15. Distribution of eigenvalues η_{nl} for phonons of a Ga 60 Å liquid drop. The lowest branch corresponds to the surface shape oscillations.

solid particle. Since the density variation of compressional oscillations satisfies Helmholtz's wave equation, the reduced eigenfrequencies are determined by the zeros of the spherical Bessel function $j_l(\eta^c_{nl})=0$. We write the eigenfrequencies as

$$ {}_c\omega_{nl}=\frac{u}{R}\eta^c_{nl} , \tag{44}$$

where u is the sound velocity of the liquid.

For a very small droplet, the shape oscillations and compressional oscillations couple with each other and the eigenvalues are determined by the equation

$$ \frac{1}{j_l(\eta)}\frac{d}{d\eta}j_l(\eta)=\frac{C}{(l-1)(l+2)}\eta , \tag{45}$$

where

$$ C=\frac{\rho R u^2}{\gamma_s} , \tag{46}$$

and the eigenfrequencies are given by $\omega_{nl}=u\eta_{nl}/R$.

We should note that extremely large C corresponds to $j_l(\eta)=0$ and extremely small C to $j_l'(\eta)=0$. This is similar to the case of Eq. (2) discussed by Balian and Bloch.[4] If η is very small, $j_l(\eta)\approx\eta^l$ and we obtain the eigenfrequencies of the surface shape oscillations represented by Eq. (43). Moreover, large l or large R yields the eigenvalues of shape oscillations for a flat surface, $\omega=\sqrt{\gamma_s/\rho}k^{1.5}$ with $l=kR$. For the details of these situations we refer to Tamura and Ichinokawa.[21] Figure 15 shows the distribution of eigenvalues for a Ga 60 Å droplet. The lowest branch corresponds to the mode of the shape oscillations. The parameters required to determine the eigenvalues are as follows: $C=194$, $\rho=6.095$ g/cm^3, $\gamma_s=707$ dyn/cm, and $u=2.74$ km/sec. In the same way as discussed in Sec. III, we define the smoothed FS by

$$ \bar{F}(\omega)\delta\omega=\sum_n(2l+1)\delta l . \tag{47}$$

We split all the modes into shape oscillation modes and compression oscillation modes by the branch number n. By the least squares method, we find the approximate expression for the reduced eigenfrequency of the shape oscillations ($n=1$)

$$ \eta=al^2+bl+c , \tag{48}$$

where the parameters are given as $a=0.006\,65$, $b=0.201$, and $c=-0.307$. By making l a continuous variable, we obtain the smoothed FS from Eq. (47) as

$$ \bar{F}_s(\eta)=\frac{1}{a}[-b+\sqrt{b^2-4ac+4a\eta}]\frac{1}{\sqrt{b^2-4ac+4a\eta}} . \tag{49}$$

For compressional oscillation modes ($n>1$), we write the reduced eigenfrequencies approximately as

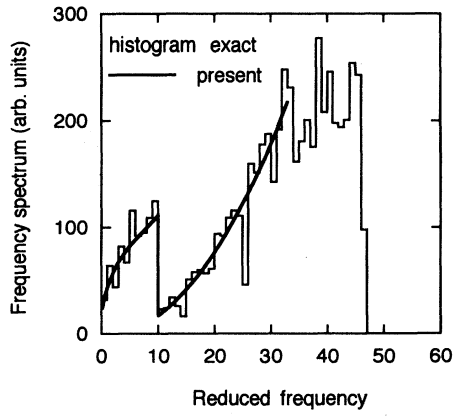

FIG. 16. Phonon FS of a Ga 60 Å liquid drop. The segment of reduced frequency is set to be 1. The peak located in the low-frequency range shows the contribution from surface shape oscillations.

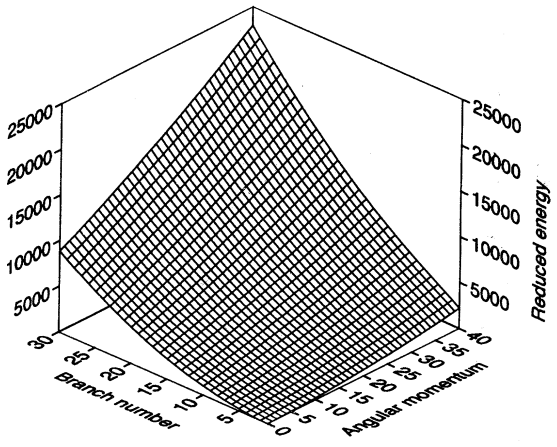

FIG. 17. 3D diagram for reduced energies η_{nl}^2 as functions of branch number n and angular momentum l. Corner points of meshes show reduced eigenenergies.

$$\eta_{nl}=\alpha l+\beta n \ . \tag{50}$$

In a similar way to Eq. (42) we find the smoothed FS of the compressional modes by

$$\bar{F}_c(\eta)=\frac{1}{\alpha^2\beta}\left[\left[\eta+\frac{\alpha}{2}\right]^2-\beta\left[\eta+\frac{\alpha}{2}\right]\right], \tag{51}$$

where $\alpha=1.22$ and $\beta=3.14$ because the relation between α and β is the same as that of Eq. (15). Figure 16 shows the FS and the peak in the low-frequency range represents the FS of the shape oscillation modes. The smoothed FS gives a good estimation of the exact FS of a droplet. This indicates that our method is applicable to a system that has a different dispersion relation from the linear combination of l and n described in Eq. (38).

VI. ENERGY SURFACE AND FREQUENCY SURFACE

From Figs. 1, 5, 11, 12, and 15 it would seem that a finite system has multivalued electron energies and phonon frequencies as a function of the good quantum number l, while the bulk system has single-valued electron energies and phonon frequencies as a function of the wave number $\mathbf{k}$. For the 3D bulk system, an electron energy is specified by three quantum numbers (n_x,n_y,n_z) which form a single-valued energy surface. For electrons of a finite system, we can construct a single-valued energy diagram as a function of n and l. We have a sheet of a curved surface in the same way as in the bulk system. Figure 17 shows a three-dimensional diagram for the energy surface. We should note, therefore, that Figs. 1 and 5 represent the projected eigenvalues on the ηl plane. The third quantum number of magnetic moment m of a spherical system gives only $(2l+1)$ overlaps at a point of the relevant energy level. With increase in the system size, the meshes in Fig. 17 become small and the energy surface becomes a smooth surface. These situations are applicable to the frequency surface of phonons.

VII. CONCLUSIONS

For several kinds of mesoscopic systems we derived the smoothed DOS of electrons and the smoothed FS of phonons. Our method is based on considering the distribution of eigenvalues, while the method by Balian and Bloch is based on the Green's function and Lorentzian smoothing. In our calculation one of the quantum numbers that specify the symmetry property of the system is made to be a continuous variable. It is shown that the present method is easily applicable to various systems and the DOS and the FS of finite systems are expressed in expanded form as inverse functions of cluster size. The general trend is explained that the DOS of a spherical particle becomes proportional to $\sqrt{E}$ and the FS becomes proportional to ω^2 with the increase in system size.

ACKNOWLEDGMENTS

This work was partly supported by the Iketani Science and Technology Foundation.

[1]W. P. Halperin, Rev. Mod. Phys. **58**, 533 (1986), and references therein.
[2]W. A. de Heer, Rev. Mod. Phys. **65**, 611 (1993), and references therein.
[3]M. Brack, Rev. Mod. Phys. **65**, 677 (1993), and references therein.
[4]R. Balian and C. Bloch, Ann. Phys. (N.Y.) **60**, 401 (1970).
[5]R. Balian and C. Bloch, Ann. Phys. (N.Y.) **63**, 592 (1971).
[6]R. Balian and C. Bloch, Ann. Phys. (N.Y.) **64**, 271 (1971).
[7]R. Balian and C. Bloch, Ann. Phys. (N.Y.) **69**, 76 (1972).
[8]V. Novotony, P. P. M. Meincke, and J. H. P. Watson, Phys. Rev. Lett. **28**, 901 (1972).
[9]V. Novotony and P. P. M. Meincke, Phys. Rev. B **8**, 4186 (1973).
[10]A. Tamura, H. Higeta, and T. Ichinokawa, J. Phys. C **15**, 4975 (1982), and references therein.
[11]K. Ohshima, A. Hayashi, and J. Harada, J. Phys. Soc. Jpn. **48**, 1631 (1980).
[12]J. Harada and K. Ohshima, Surf. Sci. **106**, 51 (1981).
[13]A. Tamura, K. Higeta, and T. Ichinokawa, J. Phys. C **16**, 1585 (1983).
[14]A. Tamura and T. Ichinokawa, J. Phys. C **16**, 4779 (1983).
[15]H. P. Baltes, J. Phys. (Paris) Colloq. **2**, 151 (1977).
[16]H. Weyl, Nachr. Akad. Wiss. Gottingen **110**, 1 (1911).
[17]H. Nishioka, K. Hansen, and B. R. Mottelson, Phys. Rev. B **42**, 9377 (1990).
[18]S. Sugano, *Microclusters,* Springer Series in Materials Science Vol. 20 (Springer-Verlag, New York, 1991), p. 148.

[19]M. Nakamura, Y. Ishii, A. Tamura, and S. Sugano, Phys. Rev. A **42**, 2267 (1990).
[20]A. A. Maradudin, E. W. Montroll, G. H. Weiss, and I. P. Ipatova, *Theory of Lattice Dynamics in the Harmonic Approximation,* 2nd ed. (Academic, New York, 1971), Suppl. 3, p. 134.
[21]A. Tamura and T. Ichinokawa, Surf. Sci. **136**, 437 (1984).
[22]A. Bohr and B. R. Mottelson, *Nuclear Structure* (Benjamin, Reading, MA, 1975), Vol. II, p. 658.